Chapter 2 Synthesis and Characterization Techniques

This chapter deals with the description of the methods used for the synthesis and characterization of rGO, MoS_2 and MoS_2-rGO heterostructure for hydrogen evolution reaction and solid-state supercapacitor applications. In the present work, we have synthesized rGO nanosheets, different morphology of MoS_2 nanostructures (nanoclusters, nanoflowers and nanosheets) and MoS_2-rGO heterostructure via hydrothermal technique and the related mechanisms have been discussed in this chapter. Fundamentals related to different characterization techniques like XRD, SEM, TEM, Raman and FTIR spectroscopy along with different electrochemical methods like linear sweep voltammetry, cyclic voltammetry, galvanostatic charge/discharge and electrochemical impedance spectroscopy techniques have been discussed in this chapter.

2.1 Materials Synthesis

Generally, two different approaches: top-down and bottom-up are used to synthesize the 2D materials, as shown schematically in **Figure 2.1**. In top-down method, separation of individual layers from bulk sample is done by compromising weak interlayer van der Waal force. Different methods like mechanical exfoliation, liquid phase exfoliation and Lithium-ion intercalation are used for the same. However, cost-effective, large area synthesis of rGO and MoS_2 nanostructures remains a challenge using these methods. In bottom-up approach, atom by atom deposition takes place and final stoichiometry is achieved to result in final compound. This approach includes the physical vapor deposition (PVD), chemical vapor deposition (CVD) and solution chemical (hydrothermal/solvothermal) process. In the present work, we have hydrothermally

synthesized rGO nanostructures using two different reducing agents (hydrazine hydrate and urea), different morphologies of MoS_2 and MoS_2-rGO heterostructure for energy generation and storage.

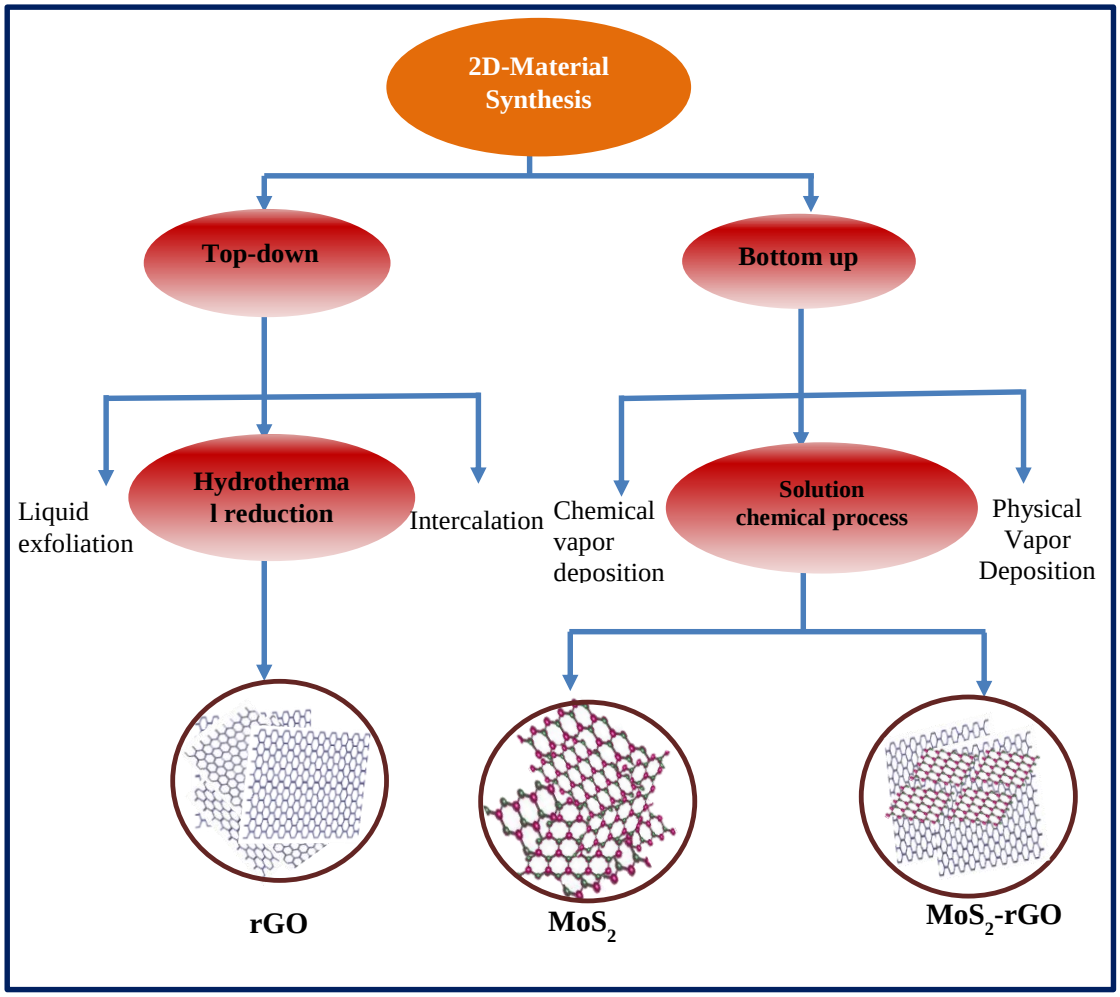

Figure 2.1 *Schematic diagram of synthesis process for 2D-nanostructures.*

2.1.1 Hydrothermal Synthesis of Nanostructures

The hydrothermal synthesis process involves synthesis in an organic or inorganic solvent in a sealed container under high pressure and temperature. The photograph of the hydrothermal cell used for synthesis of rGO, MoS_2 and heterostructure is shown in **Figure 2.2**. It consists components like stainless steel autoclave and Teflon liner. In a more traditional hydrothermal synthesis process, the reaction predominantly takes place at the interface between the precursors at moderate to high temperatures. The large quantity of

products with different morphologies can be obtained with varied time and temperature using same precursors. This process can be used to synthesis a wide variety of functionalized compounds or materials with specific shape, such as nanostructures, fine powders, or sol-gels, making it a very versatile and effective tool.

Figure 2.2 *Photograph of the used hydrothermal cell.*

2.1.1.1 Synthesis of rGO Nanostructures

In the present work, we have performed reductions of graphite oxide (GO) by the hydrothermal process using two different reducing agents. The experimental conditions for the growth of prepared rGO nanostructures are shown in **Figure 2.3**. In this work, we have initially synthesized GO by intercalating oxygen atoms using modified Hummer's method [116]. This prepared GO is further reduced by hydrothermal process to obtain final rGO samples. The schematic diagram for the synthesis of GO and rGO is shown in **Figure 2.4**.

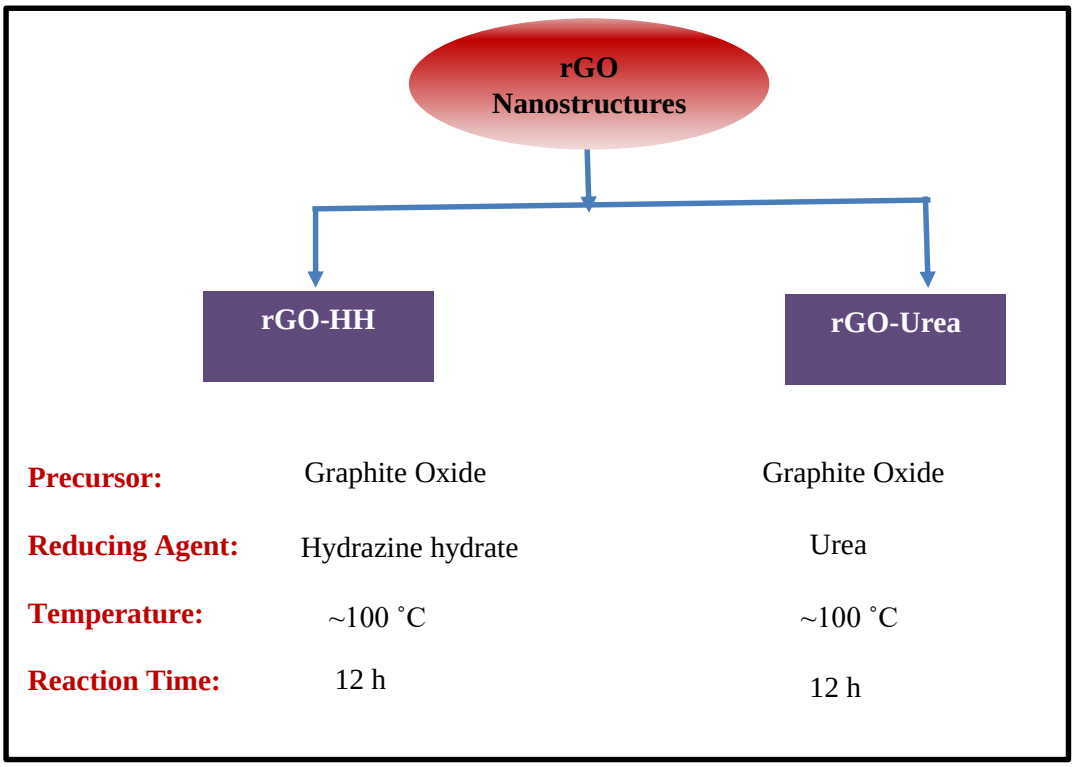

Figure 2.3 *Schematic diagram of experimental condition for synthesis of rGO nanostructures.*

In this method, pristine graphite powder (3 gm) was stirred for 10 min in the mixture of H_2SO_4 (360 mL) and H_3PO_4 (40 mL). Subsequently, $KMnO_4$ was cautiously added, and the solution was placed on a heating mantle at 50 °C to stir for 12 hours. Cooled solution mixture had been poured onto ice, and finally, 5 mL of H_2O_2 is added to remove the excess amount of $KMnO_4$, resulting in a yellow colour solution. Thereafter, prepared GO had been washed repeatedly with DI water, HCl and ethanol followed by drying at 50 °C in a vacuum oven. Further, GO was reduced using hydrazine hydrate and urea to form rGO-HH and rGO-Urea, respectively. In the typical synthesis process, 1.2 mL of hydrazine hydrate was added in 450 mg GO dispersed in 50 mL DI-water to obtain rGO-HH, while 1.2 g of urea was added separately in similar GO suspension to obtain rGO-Urea. These solutions were treated hydrothermally at 100 °C for 12 h in 100 mL Teflon-lined autoclave separately to obtain rGO-HH and rGO-Urea. The synthesized samples had been washed with DI-water and methanol to achieve pH neutral and dried at 50 °C.

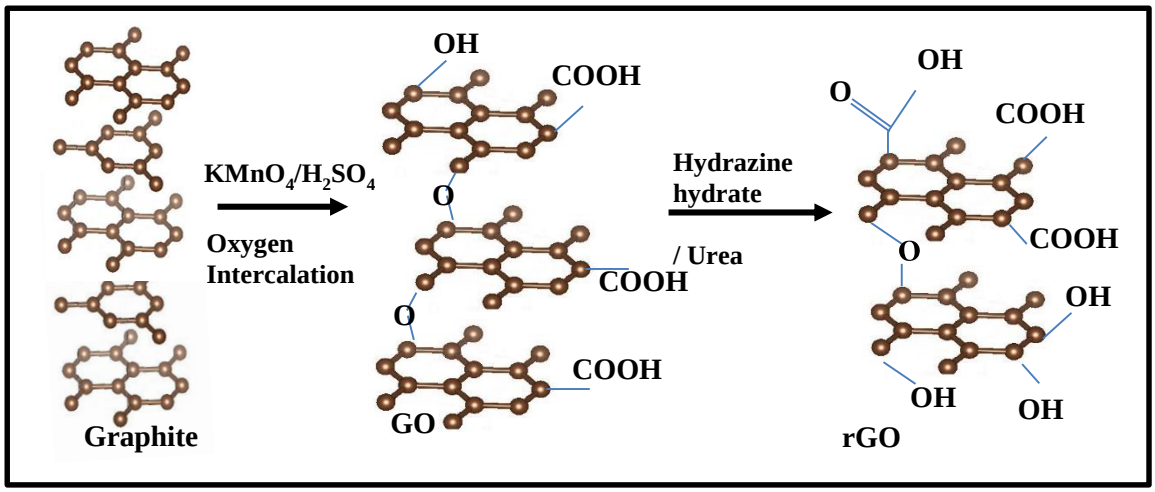

Figure 2.4 *Schematic diagram for synthesis of GO and rGO nanostructures.*

2.1.1.2 Synthesis of MoS_2 Nanostructures

We had been synthesized different morphologies of MoS_2 nanostructures (nanoclusters, nanoflowers and nanosheets) by varying the reaction time in hydrothermal process and use of additional reducing agent. We used sodium molybdate ($Na_2MoO_4 \cdot 2H_2O$) and thioacetamide (CH_3CSNH_2) powder as precursor for Mo and S source, respectively. During reaction thioacetamide reacted with DI water and form H_2S, which acts as reducing agent as well as S source. **Figure 2.5** schematically represents the synthesis conditions for three different morphologies of MoS_2 nanostructures. In a typical synthesis of MoS_2 nanostructures, 0.1 M of sodium molybdate and 0.2 M thioacetamide were subsequently dissolved in 50 mL of deionized water under stirring at room temperature. After stirring, obtained homogeneous solution was treated hydrothermally in 100 mL Teflon-lined stainless-steel autoclave at 200 °C for 24 h and 48 h to obtain MoS_2 nanoclusters and nanoflowers, respectively. The autoclave was allowed to cool naturally to the ambient temperature and obtained black precipitate had been centrifuged and washed with deionized water and ethanol to achieve pH neutrality. The washed sample was collected and dried in vacuum oven at 50 °C. In case of MoS_2 nanosheets synthesis, 2 mL of hydrazine hydrate had been used as an additional reducing agent and synthesis process

has been performed for 24 h. The presence of hydrazine hydrate provides good reduction that results in formation of crumpled sheet structures and addition of nitrogen functionality in synthesized MoS_2 nanosheets [117,118].

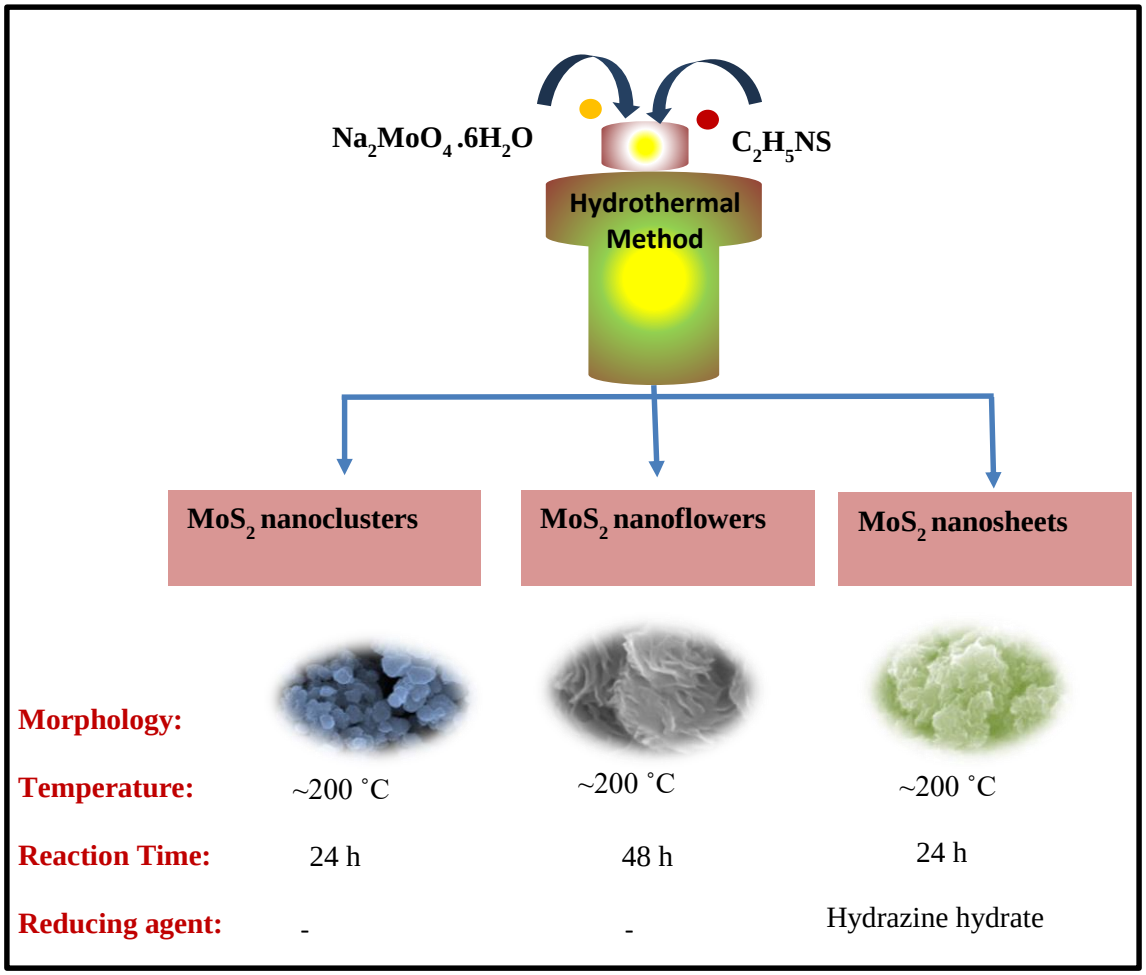

Figure 2.5 *Schematic diagram of experimental condition for the synthesis of different morphologies of MoS_2 nanostructures.*

2.1.1.3 Synthesis of MoS_2-rGO Heterostructures

To observe the synergistic effect between rGO and MoS_2 nanostructures, we have synthesized MoS_2-rGO heterostructure (1:1 ratio) using rGO along with Mo and S precursors and hydrazine hydrate as reducing agent in hydrothermal process. In the typical synthesis process 330 mg of rGO is dispersed in 50 mL DI water and stirred continuously to get homogeneous dispersion. Further, 0.1 M $Na_2MoO4{\cdot}2H_2O$, 0.2 M of CH_3CSNH_2 and 2 mL hydrazine hydrate have been dissolved in above solution. To obtain

MoS_2-rGO powder, the solution is treated hydrothermally for 24 h at 200 °C in a Teflon-lined autoclave with a capacity of 100 mL. The autoclave is allowed to cool down naturally to room temperature. The as-prepared MoS_2-rGO heterostructure is washed with DI water and ethanol in a centrifuge in sequence to achieve neutral pH and finally dried at 50 °C.

2.2 Characterization Techniques

The prepared rGO, MoS_2 and MoS_2-rGO nanostructures have been characterized by different microscopy, spectroscopy and electrochemical tools to confirm their structural, morphological and electrochemical properties. Different characterization techniques, used in the present thesis, are briefly discussed below.

2.2.1 X-ray Diffraction (XRD)

The X-ray diffraction (XRD) is one of the most popular non-destructive and non-contact material characterization techniques, that are mainly used to identify different phases, grain size, phase composition, and defect structure in the material [119]. The graph obtained by XRD is called a diffractogram, which shows the intensity as a function of angle. In the present work, XRD experiments have been performed using the Rigaku powder diffractometer - miniflex 600, which uses Cu-K_α radiation with λ=1.5406 Å, operating at 40 kV and a step size of 0.02° in the interval of 2θ (0-70°). The X-ray generator tube, sample stage and X-ray detector are three main components of XRD system. The X-rays are generated using a cathode ray tube (CRT). The high-speed electron produced by high-voltage field striking the metal object and quick deceleration of electrons on the target allows the kinetic energy of electrons to be transformed to the energy of X-ray radiation. According to Bragg's hypothesis, incident X-rays interact with sample and interferes constructively to form a diffracted ray. The detector moves in a circle around a sample following Bragg-Brentano geometry and the detector records number of X-rays (counts per

second) at different angles. The schematic diagram of XRD measurement is shown in **Figure 2.6**. Braggs' law states that the wavelength of incident radiation is proportional to the sine of angle of incidence at which the diffraction occurs, and the lattice spacing as expressed in following **equation 2.1**-

$$n\lambda = 2d \sin\theta \qquad (2.1)$$

where, n is the order of diffraction, d is the interplanar spacing, λ is the wavelength of incident ray, and 2θ is the diffraction angle. As a result, a characteristic pattern is produced, which is unique to the different crystals present in the sample and helps in identification when compared to a reference crystalline form.

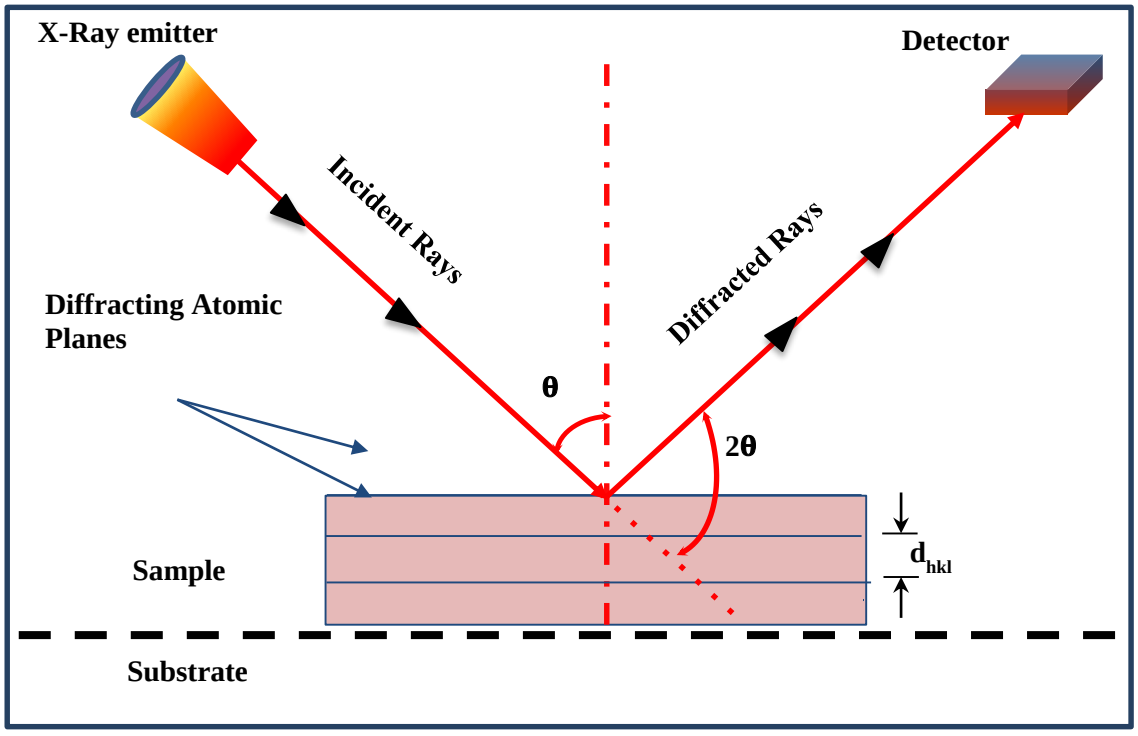

Figure 2.6 *Schematic representation of X-ray diffraction process.*

2.2.2. Scanning Electron Microscopy (SEM)

The scanning electron microscope is employed for understanding the morphological nature of the sample. The Nova NanoSEM 450 scanning electron microscope (SEM) has been used to examine at the surface morphology of as synthesized materials. In SEM technique, a high energy electron beam is focused with the help of different magnetic lens and apertures on the sample to create an image. The interaction of electron beam and sample produces different signals that determine the topography and composition of the material. The scattering process starts when a high energy electron collides with a sample, creating the secondary electrons, backscattered electrons and unique X-rays, as shown in **Figure 2.7** [119].

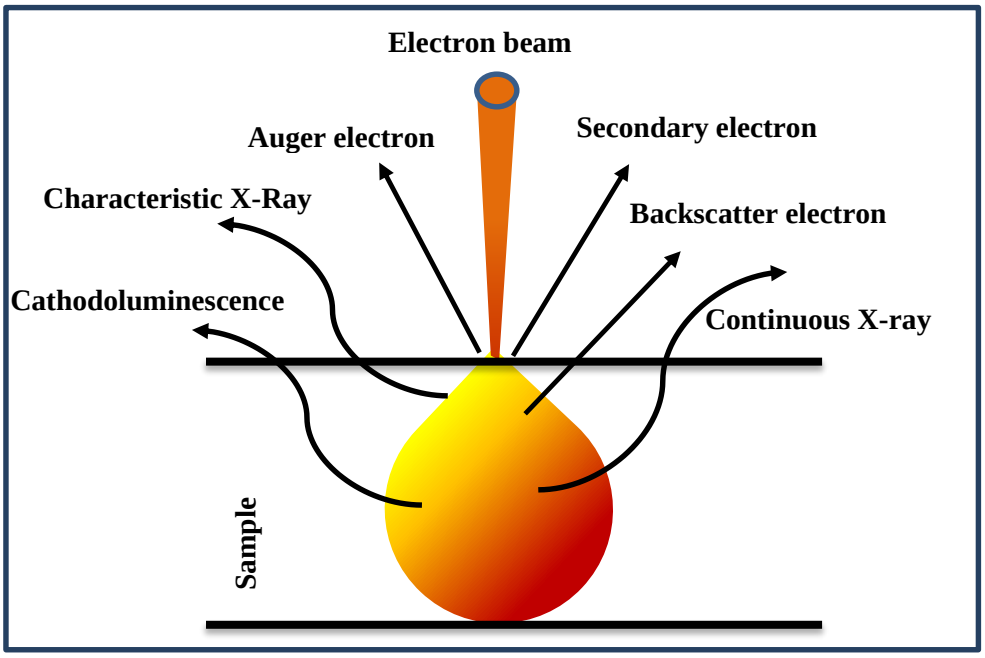

Figure 2.7 *Schematic representation of interaction of electron beam with sample in SEM.*

The emission contains information of surface topography, chemical composition and other characteristics of the sample. Secondary electrons (SE's) are produced by inelastic scattering and they consist of energy level of few KeV (interaction zone 5-50 nm) and back scattered electrons (BSEs) are produced by elastic scattering and their high energy

permits them to divert from depth about 50-300 nm. Hence, the image formed by SE's should have improved spatial resolution than image form by BSE's. Additionally, Auger electrons are also produced in low atomic number molecules. The image quality in SEM depends on the depth of field and resolution. These can be controlled by regulating operation variables such as final aperture size, the working distance, accelerating voltage, probe current, and astigmatism.

2.2.3. Transmission Electron Microscope (TEM)

Transmission electron microscopy (TEM) is a very powerful tool to characterize nanomaterials. It is an electron microscopy technique where ultrathin (less than 100 nm) sample is exposed to a high intensity electron beam to generate a two-dimensional (2D) image of the sample as shown in **Figure 2.8**.

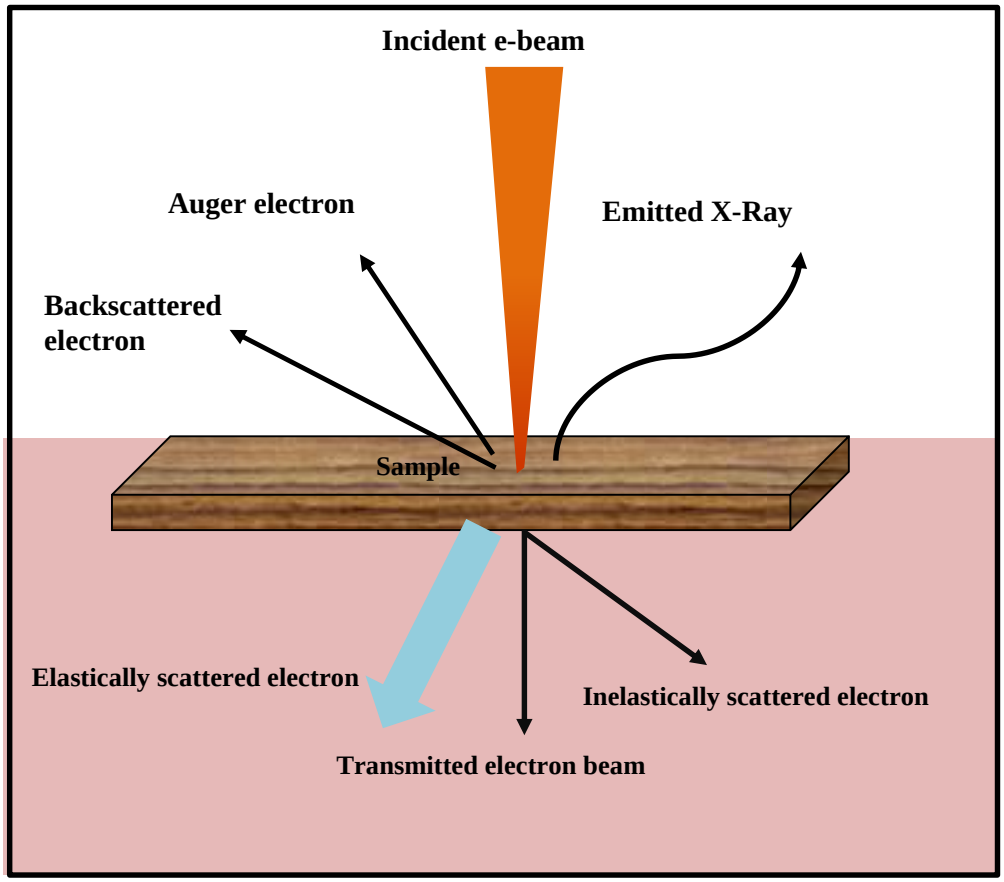

Figure 2.8 *Schematic representation of electron beam interaction with sample in TEM.*

The FEI Tecnai G2 20 TWIN TEM has been used to observed the structure, defects, number of layers and thickness of as-synthesized materials. Similar to SEM, TEM uses various magnetic lenses and apertures to focus an electron beam on the sample. The imaging in TEM is done using high energy transmitted electron beam leading to highest resolution (up to atomic level) with magnification 10 to 50 million times.

2.2.4 Raman spectroscopy

Raman spectroscopy is widely used for the analysis of vibrational features of the sample based on Raman scattering phenomena of electromagnetic radiation by molecules. Raman spectra are produced by the inelastic collision of the sample's molecules and incident monochromatic radiation.

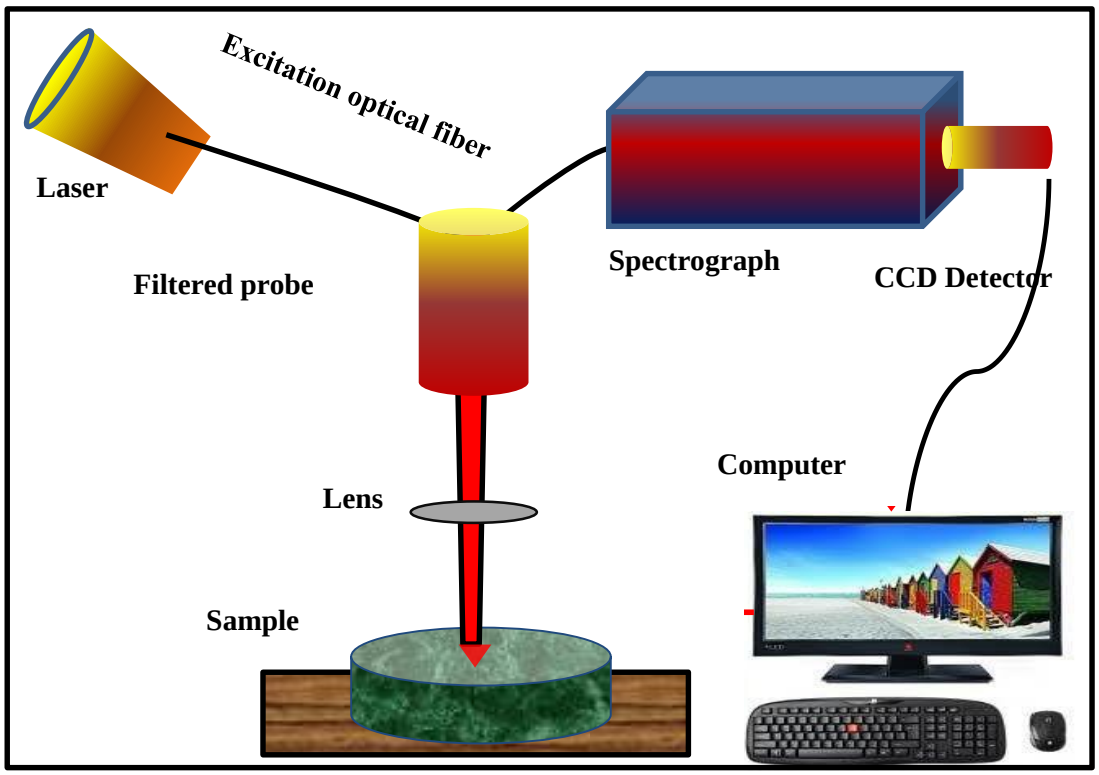

Figure 2.9 *Schematic representation of Raman spectrometer.*

We have used STR-300 micro Raman spectrometer with 532 nm laser source of power~ 1mW on the sample with a step size of ~1.2 cm^{-1}. The main components of Raman

Spectrometer are laser, sample chamber, spectrometer, and CCD detector, as shown in **Figure 2.9** [120]. Raman spectrum shows the variation of intensity of the scattered light with the wavenumber of the Raman shift i.e., the energy difference between the incident light and the scattered light.

2.2.5 Fourier Transform Infrared (FTIR) Spectroscopy

FTIR technique is used to obtain an infrared spectrum of absorption or emission of compounds. It uses the process of Fourier transform to translate the interferogram into a spectrum. The FTIR spectrum of as synthesized material has been obtained using the Thermo Fisher spectrometer (Nicolet iS5) using sample/KBr pallets. The common component of FTIR spectrometer are source, beam splitter, interferometer, sample compartment, detector, amplifier, and convertor as shown in **Figure 2.10** [121]. The radiation generated from source passes through the interferometer and sample to reach the detector. At detector, signal is amplified and converted to digital signal by A/D converter.

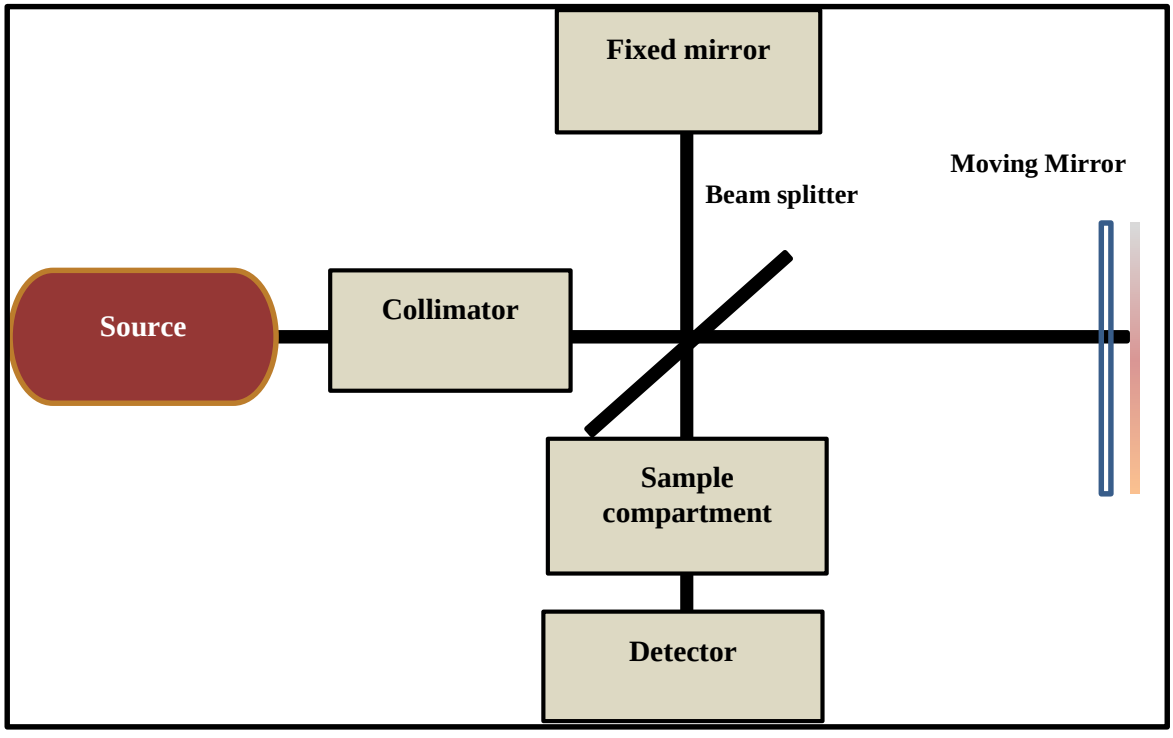

Figure 2.10 *Graphic representation of FTIR spectrometer.*

2.2.6. Electrochemical Characterization

Electrochemical characterization is used to determine the properties of electroactive materials for different applications. A three-electrode cell configuration is used to understand the electrochemical characteristics of any material. Three cell setup comprises of three electrodes: working, counter and reference electrodes. The working electrode is loaded with the electroactive material, whose properties being analyzed. The Ag/AgCl immerse in KCl is used as reference electrode, which has a constant potential drop, while platinum wire is used as counter electrode to take away generated current.

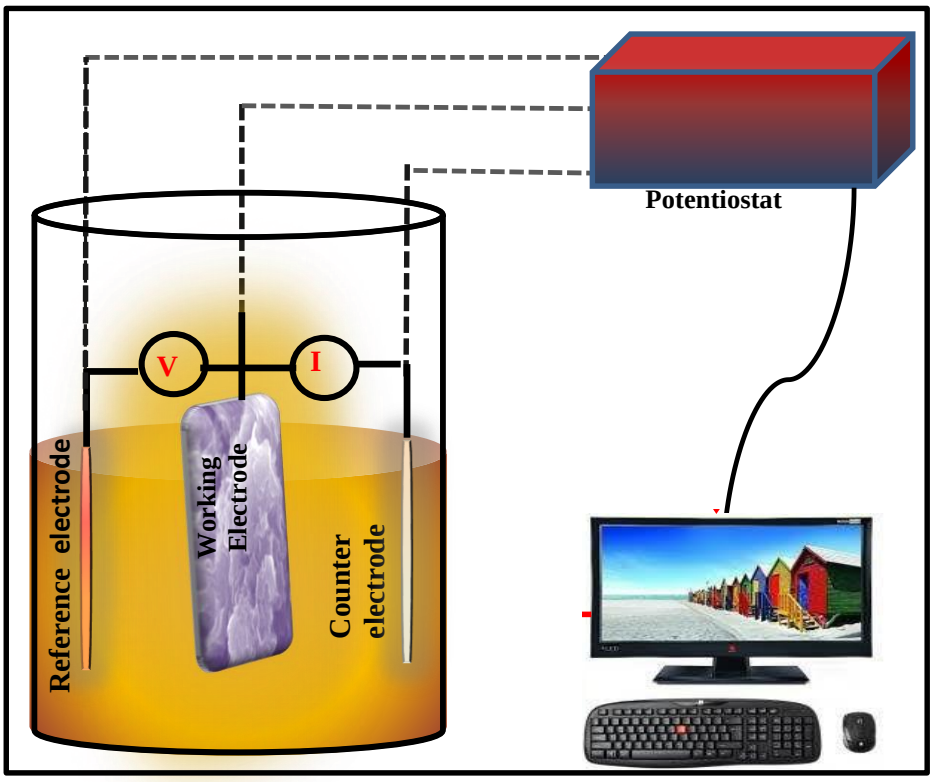

Figure 2.11 *Graphic representation of three cell electrochemical setup.*

All electrochemical measurements have been conducted using AUTOLAB (NOVA 2.0) and Corr-Test electrochemical workstations. The schematic presentation of three-cell setup for electrochemical studies is given in **Figure 2.11**. Various techniques have been devised for characterising the electrochemical performance of active materials. The most common electrochemical methods are, linear sweep voltammetry (LSV), cyclic

voltammetry (CV), galvanostatic charge-discharge (GCD) and electrochemical impedance spectroscopy (EIS), which are described below.

Linear Sweep Voltammetry (LSV)

The LSV can be used for quantitative electrochemical analysis. As indicated in the **Figure 2.12 (a)**, LSV uses a defined potential range from a lower limit to an upper limit at a constant voltage sweep rate (ν). In LSV, the potential of the electrode is varied during the reaction and the customary current is measured as a function of potential as shown in **Figure 2.12 (b)**. As the voltage sweep rate is decreased the system will take longer time to record the LSV response. As a result, the size of diffusion layer will be different depending upon the voltage scan rate i.e., at lower voltage sweep rates, ions have much time to diffuse. In the present study we have used LSV technique to evaluate the HER activity of synthesized catalysts. The drastic increment in current value indicates the good conductivity of electrode.

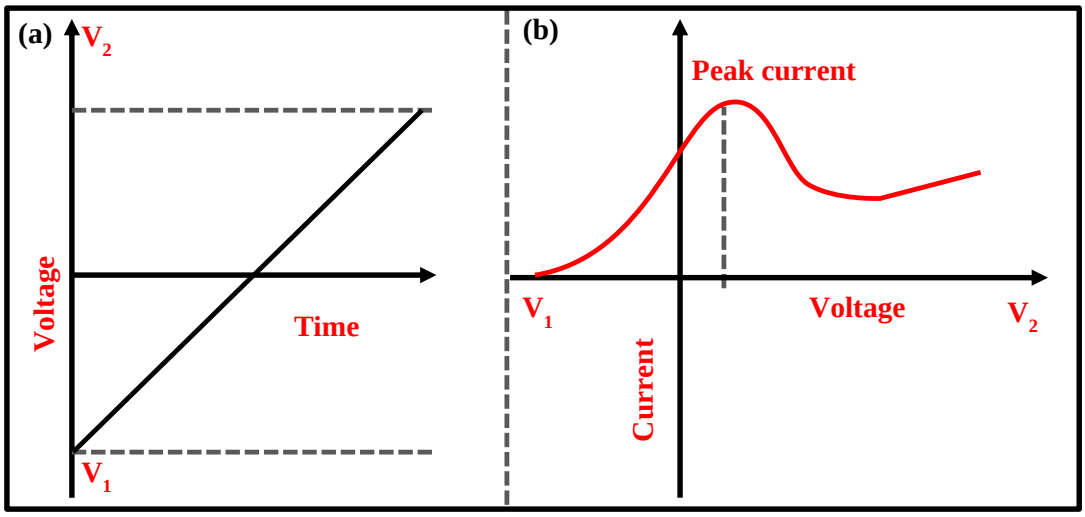

Figure 2.12 *(a) Linear voltage sweep with respect to time, (b)LSV curve at fixed voltage sweep rate.*

Cyclic Voltammetry (CV)

The CV is an effective and broadly used operative technique in electrochemistry. It determines the current that emerges in an electrochemical cell when the voltage exceeds

the value indicated by the Nernst equation. Using CV technique, qualitative and pseudo quantitative studies can be performed to determine the voltage range of the device or electrode over a wide range of scan rates. The voltage sweep rate also efficiently affects the device performance of SCs. The capacitance value increases at slower scan rate because at slower sweep rate ion diffusion has sufficient time to reach the inner pores of electrode material. The CV curve can easily differentiate the electrochemical performance of EDLCs and pseudocapacitor, as shown in **Figure 2.13**.

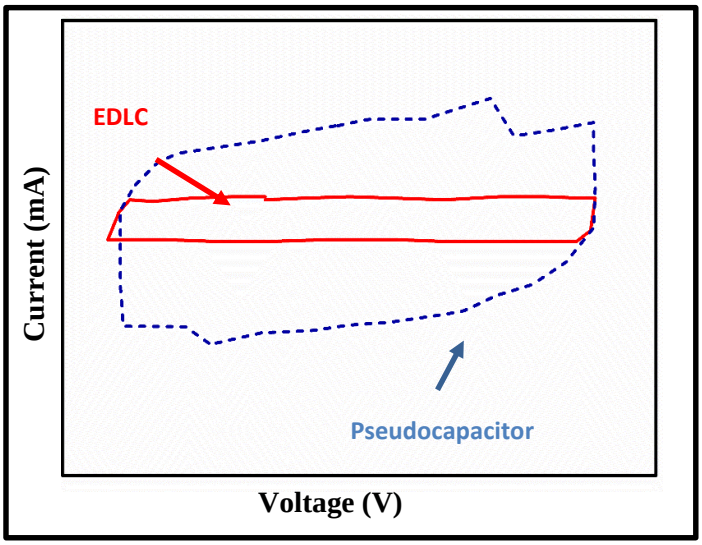

Figure 2.13 *Schematic illustration of typical CV curves for EDLCs and pseudocapacitors.*

The CV curve of EDLCs shows a rectangular shape while the pseudocapacitor have prominent redox peaks. The redox nature of pseudocapacitor has symmetric and broaden pairings which clearly differentiate the separate charge storage phenomena in pseudocapacitors. To distinguish the pseudocapacitive charge-storage process from battery, slow scan CV is utilized. The electrode kinetics can be revealed by examining the relationships between peak (i_p) current and scan rate (**v**) as per **equation 2.2** [122] -

$$\boldsymbol{i = av^b} \qquad (2.2)$$

where i is the current acquired at a certain sweep rate **ν**, a and b are variables that can be changed. In case of batteries, b= ½ and for SCs b=1 and hence EDLCs and pseudo capacitors show similar CV behaviour. The CV test is an important method to evaluate the specific capacitance value of the electrochemical cell, and it can also easily detect the degradation process of the electrode. The instantaneous voltage and current response is recorded to examine the electrochemical response.

Galvanostatic charge-discharge (GCD)

The GCD is one of the most versatile and accurate technique for characterizing electrochemical devices under direct current In GCD process, a constant current is applied until a given potential is reached and the output is plotted as potential vs time. In accordance to energy storage mechanism, at a constant discharge current, voltage vs discharge time has a linear relationship for EDLC and pseudocapacitance, as shown in **Figure 2.14**.

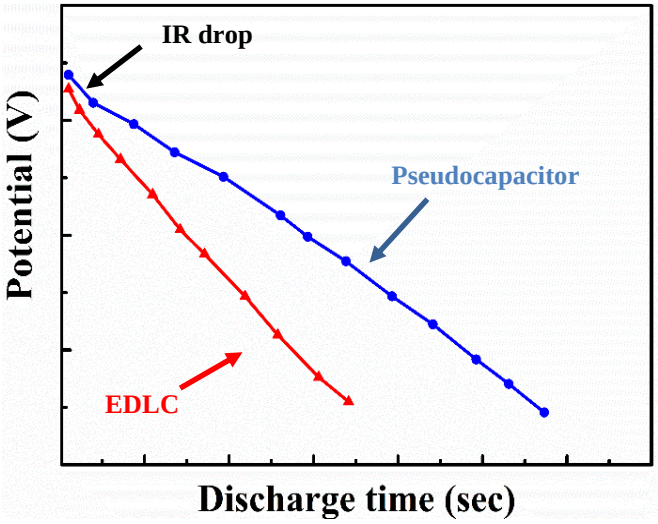

Figure 2.14 *Schematic illustration of typical GCD curves for EDLCs and pseudocapacitors.*

The pseudocapacitors have longer charge and discharge periods, indicating that more electrons and electrolyte ions are involved in the charge and discharge processes. The

EDLCs has sharper slope compared to pseudocapacitors because of its faster discharge. The linear voltage time response is described as per following **equation 2.5** [98] -

$$\boldsymbol{\Delta V \propto \Delta t} \tag{2.5}$$

where **Δ**V is the discharge potential in the given time **Δ**t. The characteristic parameters like specific capacitance, life cycle, energy and power densities are evaluated using GCD.

Electrochemical impedance spectroscopy (EIS)

EIS is an extremely sensitive and non-destructive electrochemical technique, which is used to evaluate the charge storage mechanism at the electrode/electrolyte interface. The impedance data is measured by applying a low-amplitude alternative voltage (5 to10 mV) over a wide frequencies range (0.01 to 10^6 Hz) and the results are graphically described in the form of Nyquist and Bode plots. The Nyquist plot illustrate the imaginary (Z") and real (Z′) components of the cell impedances, comprises of three separate zones an intercept on the real axis (solution resistance R_s), a semicircle in the high frequency zone (charge transfer resistance R_{ct}), and a linear component over low frequency zones (Warburg resistance W). The Nyquist plot can also be used to distinguish between EDLC and pseudocapacitance, as shown in **Figure 2.15 (a)**. The EDLC shows a vertical line (90°) from the real axis since there is absence of any Faradic process. The perfect EDLCs do not display any semicircle or ion diffusion but the practical EDLCs display a semicircle due to the presence of functionality or doping. The ideal pseudocapacitor have a very small semicircle accompanied by near vertical line where the small semi-circle depicts rapid charge transfer Faradic process [98], [123]. The Bode plot is another representation of EIS, which shows relationship between phase angle and frequency of a cell as shown in **Figure 2.15 (b)**. Bode plot is an effective technique to reveal the capacitive behaviour by simple

observation of phase shift at specified frequency values. The phase shift of nearly 90° suggests the capacitive behaviour.

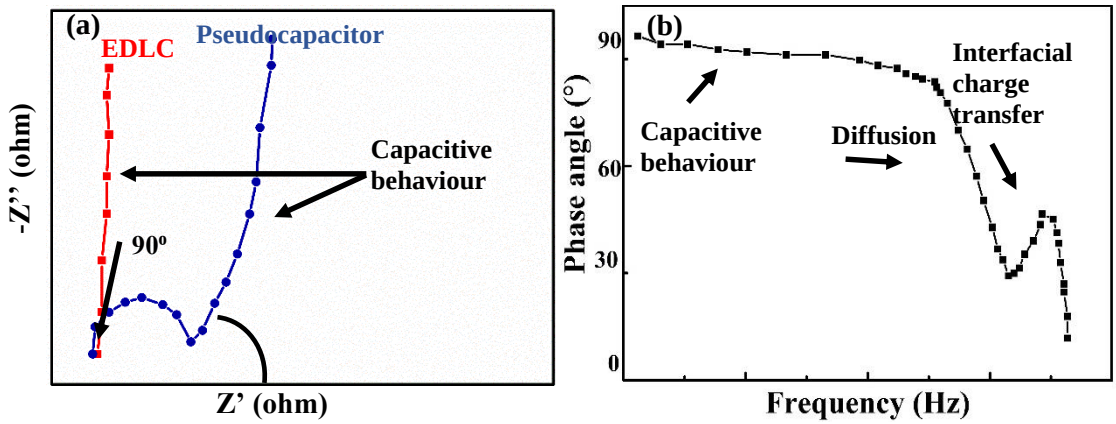

Figure 2.15 *(a) Schematic illustration of typical Nyquist plots for EDLCs and pseudocapacitors, (b) Schematic illustration of Bode Plot.*

2.2.7 Three-cell Electrochemical Measurements

To prepare the electrode, homogeneous slurry is prepared by sonication of 20 mg of as-prepared samples (rGO, MoS_2 nanostructures and MoS_2-rGO heterostructure) in 120 µL of isopropyl alcohol with 5 µL nafion binder. The conducting carbon paper of 1 cm × 1 cm area are coated using prepared slurry by brush coating method for both HER and supercapacitor tests in three-cell configuration. To reduce the binder impact, the coated electrodes have been dried overnight in a vacuum oven at 120 °C. The three-cell electrode tests have been performed with a KCl saturated Ag/AgCl as reference electrode and a Pt wire as counter electrode with a working electrode of prepared materials. The HER studies have been performed in acidic electrolyte (0.5 M H_2SO_4) using LSV at varied scan rates of 2, 5, 10 and 20 mV s^{-1} in the voltage window of 0 V to –0.7 V, where the voltage is converted to reversible hydrogen electrode (RHE). The long-term durability of HER catalyst has been evaluated using LSV measurement at sweep rate of 20 mV s^{-1} for different cycles. The EIS study for HER has been performed in a frequency interval of 0.01 Hz to 10^5 Hz at overpotential with AC amplitude of 5 mV. The capacitance measurements are

done in neutral (1M Na_2SO_4) and acidic (1M H_2SO_4) aqueous electrolytes. The CV measurements are performed at varied sweep rates from 5 to 100 mV s^{-1} within a potential range between -0.7 to 0.2 V for neutral electrolyte (1M Na_2SO_4) and -0.3 to 0.4V for acidic electrolyte (1M H_2SO_4). Galvanostatic charge/ discharge (GCD) measurements have been conducted at varied current densities (1 to 5 A g^{-1}). The EIS studies for supercapacitors have been performed in a frequency interval of 0.01 Hz to 100 kHz with AC amplitude of 5 mV.

2.2.8 Design of Hydrogen Producing Electrochemical Cell

The hydrogen production has been performed using MoS_2 nanoflowers coated carbon paper as cathode. The components of indigenously designed electrochemical cell is shown in **Figure 2.16 (a)** and the photograph of the cell is shown in **Figure 2.16 (b)**, The outer body of cell had been fabricated using acrylic sheet. The electrochemical cell comprises of cathodic and anodic compartments, where these compartments were separated by an in house manufactured separator made of PVA-H_2SO_4 gel coating over Whatman filter paper. The total cell had a capacity of 250 mL of electrolyte along with two replaceable inert electrode support structures which serve as a support to MoS_2 nanoflowers cathode and bare conducting carbon paper anode. The cathodic compartment had a gas outlet for hydrogen. The electrode assembly comprised two stainless steel supports - (4 cm ×7 cm) acting as conducting supports for electrode (2 cm × 2 cm) fixed in the center of stainless-steel supports and the electrodes are dipped in acidic electrolyte (0.5 M H_2SO_4). A DC power supply had been used to apply desired potential difference across the electrodes and the produced hydrogen is collected using downward displacement method.

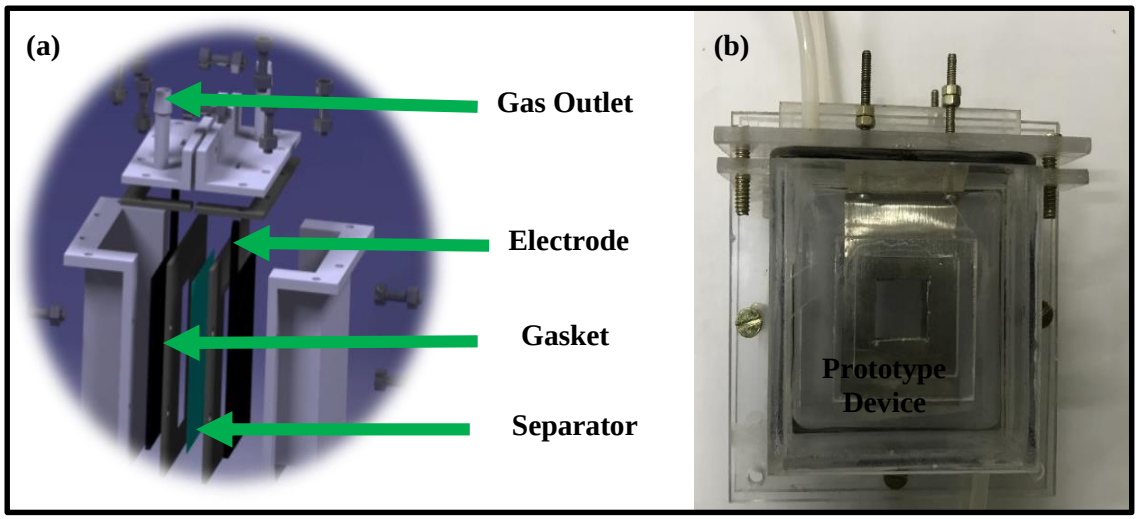

Figure 2.16 *(a) Schematic illustration of components of electrochemical cell, (b) photograph of designed electrochemical cell.*

2.2.9 Design of Solid State Supercapacitor (SSC) Device

To study the practical application, symmetric solid state supercapacitor devices have been assembled using as-prepared samples coated two identical conducting carbon electrodes of 2cm × 2cm area with neutral (PVA-Na_2SO_4) and acidic (PVA-H_2SO_4) gel electrolyte membranes. The electrodes have been prepared as discussed in previous section. The photographs of individual components of SSC device are shown in **Figure 2.17**.

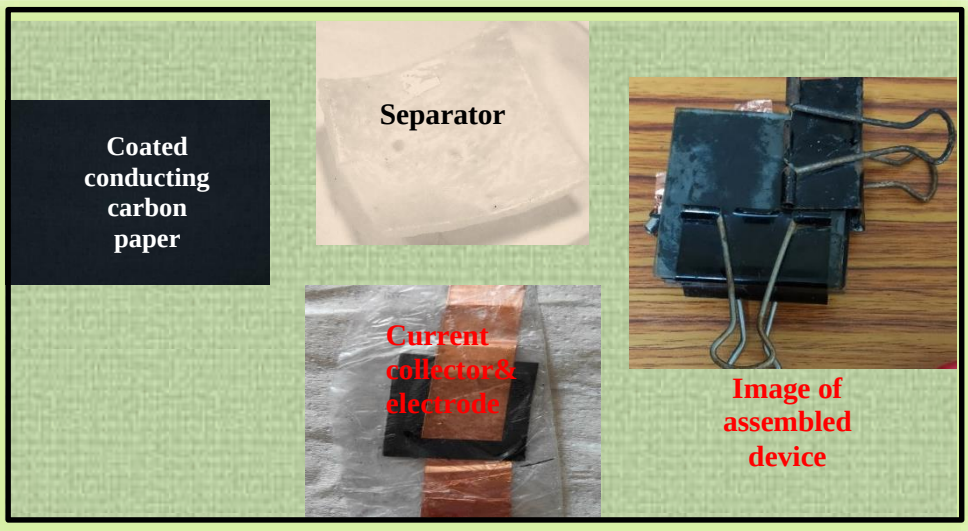

Figure 2.17 *Photographs of components of solid-state supercapacitor device.*

To prepare the PVA-Na_2SO_4 gel electrolyte, 2 g of PVA is dissolved in 30 mL deionized water at 90 °C under vigorous steering and after complete dissolution it is cooled to room temperature. Then Na_2SO_4 solution (2 g in 10 mL) is dropwise added in above solution under vigorous stirring at room temperature. The resultant solution is casted on Whatman filter paper in petri dish and subjected to cool overnight at -23°C to obtain the final solid gel PVA-Na_2SO_4 electrolyte. To prepare the PVA-H_2SO_4 gel, 2 g of PVA is dissolve in 30 mL deionized water at 90 °C under vigorous steering and 3M H_2SO_4 (10 mL) is added and stirred vigorously at room temperature. Again, the resultant solution is casted on Whatman filter paper in petri dish and subjected to cool overnight at -23°C to obtain the final solid gel PVA-H_2SO_4 electrolyte.